Quantum percolation, disorder and CMR Manganites

Alexander Weiße and Holger Fehske

Physikalisches Institut, Universität Bayreuth, Germany

UNIVERSITÄT BAYREUTH

Introduction

- In a recent attempt [1] to describe the metal-insulator transition in CMR manganites we assumed a *percolative coexistence* of two competing phases:
  - an insulating phase where doped holes are trapped by local Jahn-Teller or breathing type lattice distortions,
  - a metallic phase containing itinerant carriers whose hopping amplitude is coupled via double-exchange to a background of localized spins.

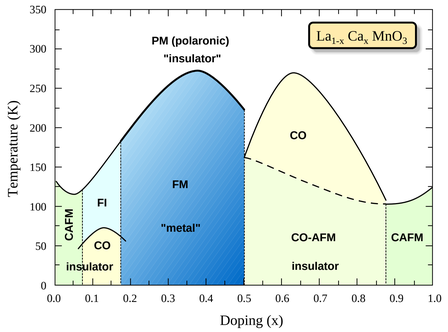

Fig. 1: Schematic experimental phase diagram for $La_{1-x}Ca_xMnO_3$ after [2].

- For the site energy in the polaronic phase we took into account the anti Jahn-Teller effect due to doping (E_1) and the polaron binding energy (E_2),

$$\varepsilon_p = \left(\frac{1}{x} - 1\right) E_1 + E_2 \,. \tag{1}$$

- The kinetic energy of the metallic phase is renormalized by the disorder of the spin background and—if insulating polaronic enclaves are sparsely embedded—by the irregular shape of the metallic cluster. As a simplified approximation we considered

$$\varepsilon_f(\mathbf{k}) = p^{(f)} \gamma_{\bar{S}}[\bar{S}\lambda]\, \varepsilon_0(\mathbf{k}) \,, \tag{2}$$

where $\varepsilon_0(\mathbf{k})$ denotes some bare band and $p^{(f)} = \frac{N^{(f)}}{N}$ is the volume fraction occupied by the metallic phase. In an ordering field $\lambda = \beta g \mu_B h_{\text{eff}}$ the spin background contributes [3],

$$\gamma_{\bar{S}}[z] = \tfrac{1}{2} + \tfrac{\bar{S}}{2\bar{S}+1} \coth(\tfrac{2\bar{S}+1}{2\bar{S}} z) \left[\coth(z) - \tfrac{1}{2\bar{S}} \coth(\tfrac{z}{2\bar{S}})\right] \,. \tag{3}$$

- Assuming equal hole density in both phases,

$$x = \frac{N_h}{N} = \frac{N_h^{(f)}}{N^{(f)}} = \frac{N_h^{(p)}}{N^{(p)}} \,, \tag{4}$$

the size of the metallic phase, and hence the electronic bandwidth, is coupled self-consistently to the number of itinerant carriers. Minimizing the total free energy with respect to λ, for characteristic parameter sets we obtained the phase diagrams:

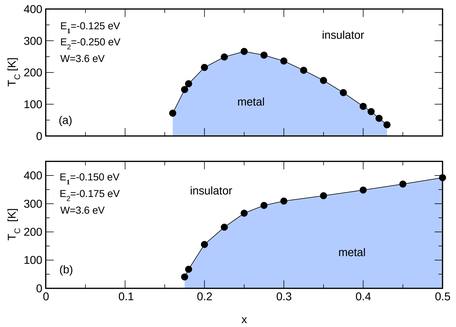

Fig. 2: Phase diagram of the metal-insulator transition within two-fluid model [1].

Quantum percolation model

Since the above approximation (2) for the metallic phase is rather simplified, we study percolative aspects and disorder in more detail. Namely, we consider the classical double-exchange model on a site percolated cluster,

$$H = \sum_{\langle kl \rangle} [t_{kl} c_k^\dagger c_l + \text{H.c.}] \,. \tag{5}$$

Here $c_l^\dagger$ creates a spinless fermion in the Wannier state at site l, and the summation is over neighboring sites on a simple cubic lattice.

- Given a probability p, sites of a simple cubic lattice are chosen randomly. Only within the largest classically percolated cluster spinless fermions are allowed to hop with amplitude [4]

$$t_{kl} = \cos\tfrac{\theta_k}{2} \cos\tfrac{\theta_l}{2}\, e^{-i(\phi_k - \phi_l)/2} + \sin\tfrac{\theta_k}{2} \sin\tfrac{\theta_l}{2}\, e^{i(\phi_k - \phi_l)/2} \,. \tag{6}$$

- The set of angles $\{\theta_l, \phi_l\}$ parameterizes the background of classical spins. It is taken from an ensemble of thermalized classical spins in a magnetic field h_{eff}. This introduces the parameter $\lambda = \beta g \mu_B h_{\text{eff}}$.
- Hence, in the present model there are two types of disorder which cause scattering or localization of the involved fermions:
  - the random structure of the cluster and
  - the disorder in the hopping matrix elements.

Density of states

The density of states (DOS),

$$\rho(E) = \sum_n \delta(E_n - E) \,, \tag{7}$$

of the above free fermion model can be calculated very accurately with the aid of Chebyshev expansion and maximum entropy methods [6].

- For the ordered spin background ($\lambda = \infty$) with decreasing p a pseudo-gap feature appears close to the band center, together with a distinct peak at $E = 0$. The weight W of this central peak (left hand inset) increases continuously, and makes up more than 10% of the spectrum close to the classical percolation threshold $p_c \approx 0.3116$. Increasing spin disorder, i.e., decreasing λ, transfers spectral weight to the band center. However, this does not seem to affect the weight of the central peak. Of course, both types of disorder reduce the overall bandwidth.

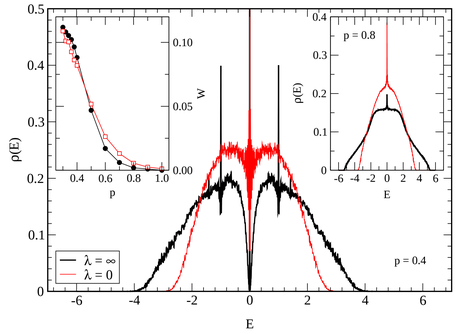

Fig. 3: Density of states calculated on a 100^3 site lattice for $p = 0.4,\ 0.8$ and $\lambda = 0,\ \infty$; Left inset: weight of the central peak.

- The states in the band center show a typical chequerboard structure (left) compared to the states from other parts of the spectrum (right) (cf. also [7]).

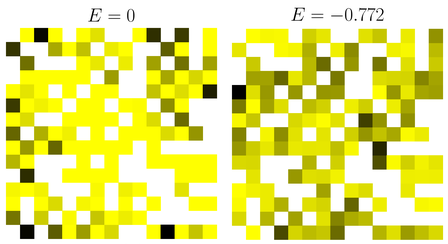

Fig. 4: Amplitude $|\phi|$ of the free fermion wave function on a slice of a 15^3 site cube.

Localization

To obtain information about localization properties of the model, we consider the *typical* density of states (TDOS) [8], which is defined as the geometric mean of the *local* density of states (LDOS),

$$\rho_i(E) = \sum_n |\phi_i^n|^2 \delta(E_n - E) \,, \tag{8}$$

$$\rho_{\text{typ}}(E) = \exp\left(\langle \log[\rho_i(E)] \rangle\right) \,. \tag{9}$$

Here ϕ_i^n denotes the amplitude of the free fermion state n at site i.

- Using the above numerical methods to compare DOS and TDOS for the case $p = 1$, we observe that disorder of the spin background alone is not sufficient for localization. Band and mobility edge almost coincide.

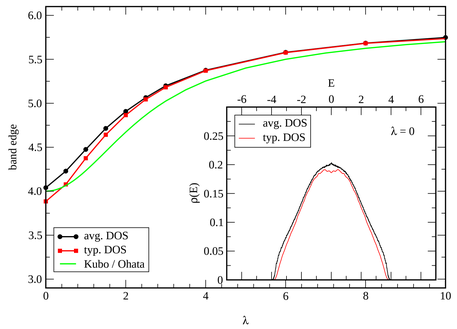

Fig. 5: Band and mobility edge versus spin disorder; Inset: DOS and TDOS for fully disordered spin background ($p = 1$, $N = 64^3$).

- The situation changes drastically for diluted clusters. TDOS is noticeable reduced and below $p \lesssim 0.38$ vanishes at the band center. Interestingly, the distinct peaks visible in DOS do not contribute to TDOS.

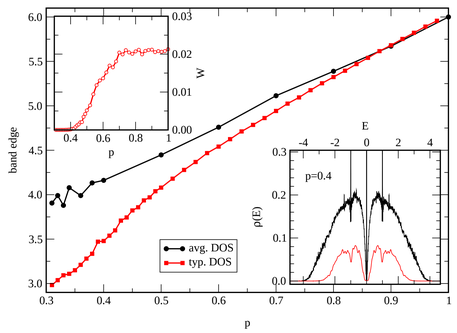

Fig. 6: Band and mobility edge versus probability p; Insets: DOS & TDOS at $p = 0.4$ and drop of TDOS at $E = 0$ ($\lambda = \infty$, $N = 64^3$).

Optical conductivity

Additional information about the model can be obtained, considering its optical properties, namely the regular part of the optical conductivity,

$$\sigma_{\text{reg}}(\omega) = \frac{1}{N} \sum_{m \neq 0} \frac{|\langle m | j_x | 0 \rangle|^2}{\omega_m} \delta(\omega - \omega_m) \,, \tag{10}$$

with $\omega_m = E_m - E_0$. The current j_x is given by

$$j_x = \sum_{\langle kl \rangle_x} [i\, t_{kl} c_k^\dagger c_l + \text{H.c.}] \,, \tag{11}$$

where the summation extends over neighboring sites in x-direction only.

Considering clusters on a 10^3 site lattice, we calculated the eigenstates of the hopping matrix and summed up the current matrix elements between empty and occupied eigenstates. We assumed zero (electron) temperature and a band filling of $x = 0.2$.

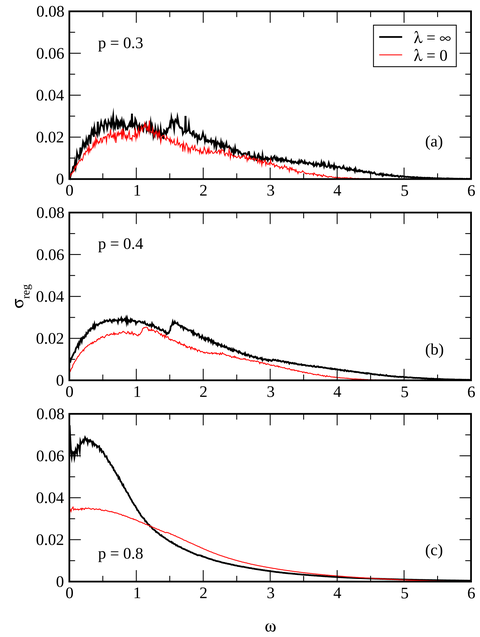

Fig. 7: Optical conductivity for $p = 0.3,\ 0.4,\ 0.8$ and $\lambda = 0,\ \infty$ averaged over 700 realizations on a 10^3 site lattice.

Clearly, below the classical percolation threshold (panel (a)) we deal with finite size clusters which do not (or rarely) connect the boundaries. Hence, the averaged σ_{reg} is rather noisy and approaches zero in the limit $\omega \to 0$. For $p > p_c$ (panels (b) and (c)) the curves become smooth, and we obtain a finite dc conductivity. In panel (b) the hump between $\omega = 1$ and 2 is due to excitations into the central peak. With decreasing λ it is shifted to lower frequencies, because of the reduced bandwidth. Further studies of the model should clarify whether a quantum percolation threshold [9] $p_q > p_c$ is visible in the optical conductivity.

References

[1] A. Weiße, J. Loos, and H. Fehske, Phys. Rev. B **64**, 054406 (2001); *ibid.*, 104413 (2001).

[2] P. Schiffer *et al.*, Phys. Rev. Lett. **75**, 3336 (1995) and other.

[3] K. Kubo and N. Ohata, J. Phys. Soc. Jpn. **33**, 21 (1972).

[4] P. W. Anderson and H. Hasegawa, Phys. Rev. **100**, 675 (1955); E. M. Kogan and M. I. Auslender, Phys. Status Solidi B **147**, 613 (1988).

[5] J. Hoshen and R. Kopelman, Phys. Rev. B **14**, 3438 (1976).

[6] R. N. Silver and H. Röder, Phys. Rev. E **56**, 4822 (1997).

[7] M. Inui, S.A. Trugman, and E. Abrahams, Phys. Rev. B **49**, 3190 (1994).

[8] V. Dobrosavljević, A.A. Pastor, and B.K. Nikolić, cond-mat/0106282; M. Janssen, Phys. Rep. **295**, 1 (1998).

[9] A. Kaneko and T. Ohtsuki, J. Phys. Soc. Jpn. J. **68**, 1488 (1999) and references therein.